

Electronic Supplementary Information

Exceptionally enhanced Raman Optical Activity (ROA) of amyloid fibrils and their prefibrillar states

Aleksandra Kolodziejczyk^{a,b}, Laurence A. Nafie^c, Aleksandra Wajda^{a*} and Agnieszka Kaczor^{a*}

^a Faculty of Chemistry, Jagiellonian University, Gronostajowa 2, 30-387 Krakow, Poland.

^b Doctoral School of Exact and Natural Sciences, Jagiellonian University Lojasiewicza 11, 30-348 Krakow, Poland.

^c Department of Chemistry, Syracuse University, Syracuse, New York, USA, 13244

Contents

1. Experimental

- 1.1. Preparation of fibrils
- 1.2. Raman Optical Activity (ROA)
- 1.3. Vibrational Circular Dichroism (VCD)
- 1.4. Electronic circular dichroism (ECD) and Linear Dichroism (LD)
- 1.5. Transmission Electron Microscopy (TEM)
- 1.6. Comparison of the results with previous data on ROA of fibrils and prefibrillar states

2. Tables and figures

Table S1. Approximate values of Circular Intensity Difference (CID) for HEWL and HL protofibrils and fibrils.

Table S2. Evaluation of the protein secondary structure for HEWL and HL fibrils based on BeStSel (Beta Structure Selection).

Figure S1. ROA and VCD of insulin fibrils before and after sonication.

Figure S2. TEM of fibril samples.

Figure S3. Evaluation of anisotropy in fibril samples.

Figure S4. Separate Raman and ROA spectral blocks for HEWL early-stage and mature fibrils.

Figure S5. Evolution of the ROA, VCD and ECD signals during formation of HL fibrils.

Figure S6. Evolution of the Raman, IR and electronic absorption spectra during HEWL formation.

Figure S7. Evolution of the Raman, IR and electronic absorption spectra during HL formation.

Figure S8. Repetition of the time evolution experiment for HEWL.

Figure S9. Electronic absorption, IR, Raman, ECD, VCD and ROA spectra of mature insulin fibrils.

Figure S10. Electronic absorption, IR, Raman, ECD, VCD and ROA spectra of HL fibrils obtained at the quiescent conditions.

Figure S11. Comparison of amyloid fibril Raman spectra (A): insulin (0 rpm), HEWL (1400 rpm) and HL (1400 rpm). Respective ROA spectra of native proteins are given for reference (B).

Figure S12. ROA of HEWL fibrils with the inset showing more clearly the enhancement in the lower frequency range.

1. Experimental

1.1. Preparation of fibrils

Hen egg white and human lysozymes

Fibrils were prepared according to the previous reports¹⁻³, yet with the application of agitation⁴ to accelerate fibrils' formation. 60 mg of hen egg white lysozyme powder (Bioshop, HEWL) and 60 mg of human lysozyme powder (Sigma-Aldrich, HL) were dissolved in 6 mL of ultrapure water. The pH was adjusted by HCl to a final pH of 2.0. The samples were divided into portions of 0.5 ml and set in eppendorfs. Due to a different heat transfer for different volumes of the sample, affecting kinetics of the fibril formation, we decided to carry on fibrilization in exactly the same conditions, including the volume of the sample. Therefore, fibrils at every time point were obtained from the same native solution, in exactly the same conditions, in particular at exactly the same effective temperature inside the eppendorf. Samples were incubated in the thermomixer TS-100 Biosan up to 12 hours at 60°C with agitation (1400 rpm).

HL fibrils were prepared also without agitation, via dissolving of 60 mg of human lysozyme powder (Sigma-Aldrich, HL) in 1 mL of ultrapure water. The pH was adjusted by HCl to a final pH of 2.0. The sample was incubated in the thermomixer TS-100 Biosan 96 hours at 60°C without agitation (0 rpm).

Insulin

60 mg of bovine pancreas insulin (Sigma-Aldrich) was dissolved in 1mL of ultrapure water. The pH was adjusted by HCl to a final pH of 2.0. The sample was incubated in the thermomixer TS-100 Biosan up to 3 hours at 70°C without agitation (0 rpm).

All experiments presented here were repeated at least twice, for time evolution experiments different time points were repeated three times using different time points.

1.2. Raman Optical Activity (ROA)

ROA spectra were measured in the optical cells with anti-reflective coating with dimensions of 3x4 mm, in the 250-2550 cm^{-1} spectral range using ChiramRAMAN-2XTM spectrometer with a 532 nm excitation wavelength and 7 cm^{-1} spectral resolution. Laser power of 700 mW and integration time of 0.8-2 s were used. Total acquisition time for ROA/Raman depended on the sample and it was: for agitated lysozyme fibrils typically 1-2 h, for non-agitated fibrils ca. 18-20 h and for native proteins up to 4 days. The ROA/Raman spectra were collected and saved in 5 min blocks. The final spectra were averaged over all blocks. To analyze Raman and ROA spectra OriginPro 2022 9.9.0.220 (Academic) Copyright OriginLab Corporation 1991-2021 was used.

OPUS 7.2 [Build: 7, 2, 139, 1294] Copyright Bruker Optik GmbH 2012 was used to do the interactive baseline correction. Approximately 9 baseline points were set manually and the polynomial baseline was adjusted to the original ROA/Raman spectrum.

1.3. Vibrational Circular Dichroism (VCD)

FTIR and VCD were measured using ChiralIR-2XTM, BioTools. The samples were placed between two CaF_2 windows (BioCell, 6 μm pathlength) and the data were collected for ca. 2 h or 14 h for fibrils and native protein, respectively. The spectra were obtained at room temperature with a spectral resolution of 8 cm^{-1} . The spectra were processed in OPUS 7.2 [Build: 7, 2, 139, 1294] Copyright Bruker Optik GmbH 2012 and OriginPro 2022 9.9.0.220 (Academic) Copyright OriginLab Corporation 1991-2021. pH

2.0 solvent spectra were subtracted as background. Baseline was corrected using a first-order polynomial.

1.4. Electronic circular dichroism (ECD) and Linear Dichroism (LD)

UV-vis, ECD and LD spectra were measured in quartz cells with a path length of 0.2 mm, in the 190-300 nm spectral range using the Jasco J-815 spectrometer. The spectra were recorded using 50 nm/min scanning speed, 1 nm bandwidth, and 0.2 nm data pitch, by averaging 5 scans. The samples were diluted approximately 400 times.

For the analysis of UV-vis, ECD and LD spectra, JASCO version 1.52.00 [Build 4] Copyright JASCO Corporation 1995-2000, OPUS 7.2 [Build: 7, 2, 139, 1294] Copyright Bruker Optik GmbH 2012, and OriginPro 2022 9.9.0.220 (Academic) Copyright OriginLab Corporation 1991-2021 software were used. The spectra were background-corrected using the spectra of the solvent at pH 2. The identification of the secondary structures in the obtained fibrils were estimated based on the ECD data (range 190–250 nm) using BeStSel (Beta Structure Selection) algorithm^{5,6}.

1.5. Transmission Electron Microscopy (TEM)

Before TEM analysis, all samples were diluted 10 times. For negative staining the copper grid coated with formvar and carbon were used. Samples were incubated during 3 min on grids. After that time the excess was drained using piece of filter paper. Next, grids were washing on two drops of the distilled water and uranyl acetate. After rinsing grids were left on drop of uranyl acetate over 1 min and then they were dried in the air.

For observation, the JEOL JEM 2100HT electron microscope (Jeol Ltd, Tokyo, Japan) was used at accelerating voltage 80 kV. Images were taken by using 4kx4k camera (TVIPS) equipped with EMMENU software ver. 4.0.9.87.

1.6. Comparison of the results with previous data on ROA of fibrils and prefibrillar states

As the results that we present are different than those published previously, below we express our opinion why the previous measurements did not manage to show the enhanced ROA.

Blanch et al¹, according also to their own conclusions, measured prefibrillar states and did not observe significant enhancement, what is not unexpected and what we have also described in our work (vide Fig. 1, main text, the inset in the right panel).

Yamamoto and Watarai⁷ did not measure the fibrils as they were obtained, but measured samples that were sonicated. Sonication is well-known to change significantly the structure of amyloid fibrils (reduce in size, increase solubility)⁸⁻¹¹, what is confirmed by the authors' observation that the samples recorded after 14 h from the formation of the amyloid showed ROA as for the native protein (ref. 7, Fig. 2, bottom panel).

Additionally, in the previous works, no reference methods were used (apart from ECD, that just showed α -helix $\rightarrow\beta$ sheet reorganization in the Yamamoto and Watarai's work). To confirm that we formed fibrils, we used TEM and VCD, apart from ECD.

Moreover, in the previous work, the fibrils of only one protein was measured and fibril formation was not documented using any microscopic methods, but we show results for three different proteins and confirm them via analyzing LD/ECD depending on orientation, separate ROA blocks etc.

Our experiments, therefore, seem rather straightforward compared to the previous ones. We did not mix samples, neither did we use sonication. Our measurements using ROA, VCD, ECD and TEM were performed for fibrils as they were formed. We repeated our experiments obtaining qualitatively the same results and we did several additionally analysis to exclude the possibility of the birefringence artifacts, what is confirmed by the repeatability of the ROA signal for the measured samples, the lack of influence of orientation on the ECD signal and lack of LD as well as the analysis of single blocks.

To repeat Yamamoto and Watarai's experiment⁷, we have obtained the insulin fibrils via incubation at 70-80°C of the aqueous insulin solution of the initial concentration of 60 mg ml⁻¹ at pH 2.0 without agitation for 4 h and measured ROA and VCD for this sample and then applied sonication (in ultrasound bath for 90 minutes) and then measured again the sonicated sample. As the Figure S1 shows, the intense VCD and ROA obtained after fibril formation is dramatically decreased.

2. Tables and figures

Table S1. Approximate values of the Circular Intensity Difference (CID) for HEWL and HL protofibrils and fibrils.

| HEWL | | | | | | | | | |
|-------------------------|----------------------|-----------------------|-----------------------|-----------------------|-----------------------|-----------------------|------------------------|-----------------------|------------------------|
| 3h | 4h | 5h | 6h | 7h | 8h | 9h | 10h | 11h | 12h |
| 1.5·10 ⁻³ | 5.1x10 ⁻² | 1.5·10 ⁻¹ | 5.1·10 ⁻² | -5.5·10 ⁻⁴ | 4.3·10 ⁻³ | -3.6·10 ⁻³ | - 9.5·10 ⁻³ | -7.3·10 ⁻² | - 6.6·10 ⁻² |
| HL | | | | | | | | | |
| 3h | 4h | 5h | 6h | 7h | 8h | 9h | 10h | 11h | 12h |
| - | 2.3·10 ⁻² | -4.6·10 ⁻³ | -9.7·10 ⁻³ | 2.1·10 ⁻² | -3.8·10 ⁻² | 2.3·10 ⁻² | 9.4·10 ⁻³ | -1.2·10 ⁻² | 1.6·10 ⁻² |
| insulin | | | | | | | | | |
| 3h | | | | | | | | | |
| -8.6 · 10 ⁻³ | | | | | | | | | |

Table S2. Evaluation^a of the protein secondary structure for HEWL and HL fibrils based on BeStSel^{5, 6} (Beta Structure Selection).

| Secondary structure (↓↑ROA) | HEWL | | | HL | | |
|--------------------------------|-------------|---------------------------|---------------------------|-------------|---------------------------|---------------------------|
| | 3h - | Average ^b ↑ | Average ^b ↓ | 3h - | Average ^b ↑ | Average ^b ↓ |
| Helix | 33.4 | 22.2 | 21.1 | 27.2 | 17.4 | 14.6 |
| Helix 1 (regular) | 19.3 | 16.9 | 17.9 | 16.1 | 11.4 | 10.4 |
| Helix 2 (distorted) | 14.2 | 5.3 | 3.2 | 11.0 | 6.0 | 4.2 |
| Antiparallel | 9.6 | 19.8 | 22.2 | 12.3 | 20.0 | 26.0 |
| Anti 1 (left-twisted) | 0.0 | 1.7 | 3.9 | 1.0 | 3.1 | 5.9 |
| Anti 2 (relaxed) | 2.9 | 8.7 | 9.8 | 4.6 | 8.5 | 10.8 |
| Anti 3 (right-twisted) | 6.7 | 9.4 | 8.5 | 6.7 | 8.5 | 9.3 |
| Parallel | 5.3 | 15.0 | 19.1 | 5.5 | 15.2 | 14.4 |
| Antiparallel+Parallel | 14.9 | 34.9 | 41.3 | 17.8 | 35.2 | 40.4 |
| Turn | 8.6 | 7.0 | 5.0 | 12.0 | 8.8 | 7.5 |
| Others | 43.0 | 36.0 | 30.4 | 43.0 | 38.6 | 37.5 |

^aas the concentration of 60 mg/ml was assumed for all samples, the results should be considered very approximate, ^bthe results were averaged for fibril spectra showing the same ROA sign to highlight the changes.

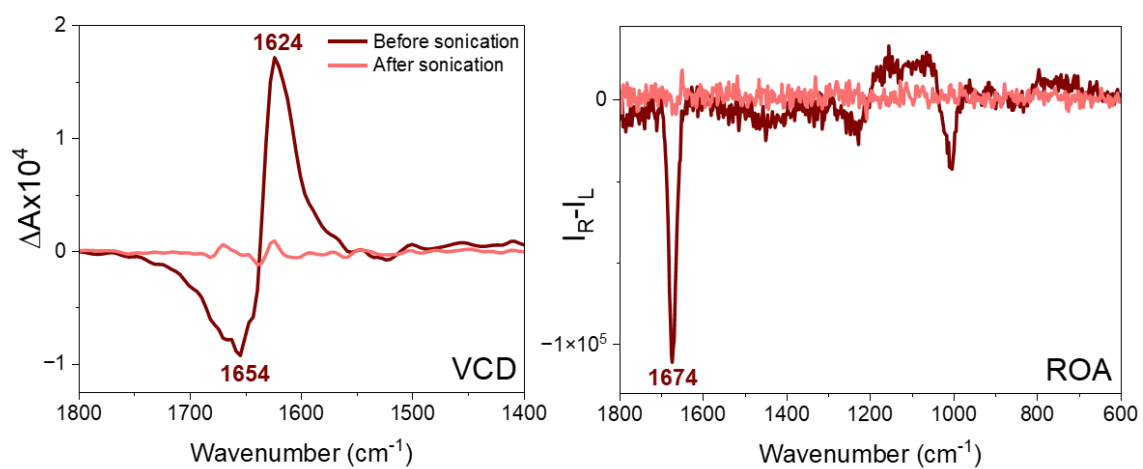


Fig. S1. ROA and VCD of insulin fibrils before and after sonication. The conditions of the measurements were the same for samples before and after sonication.

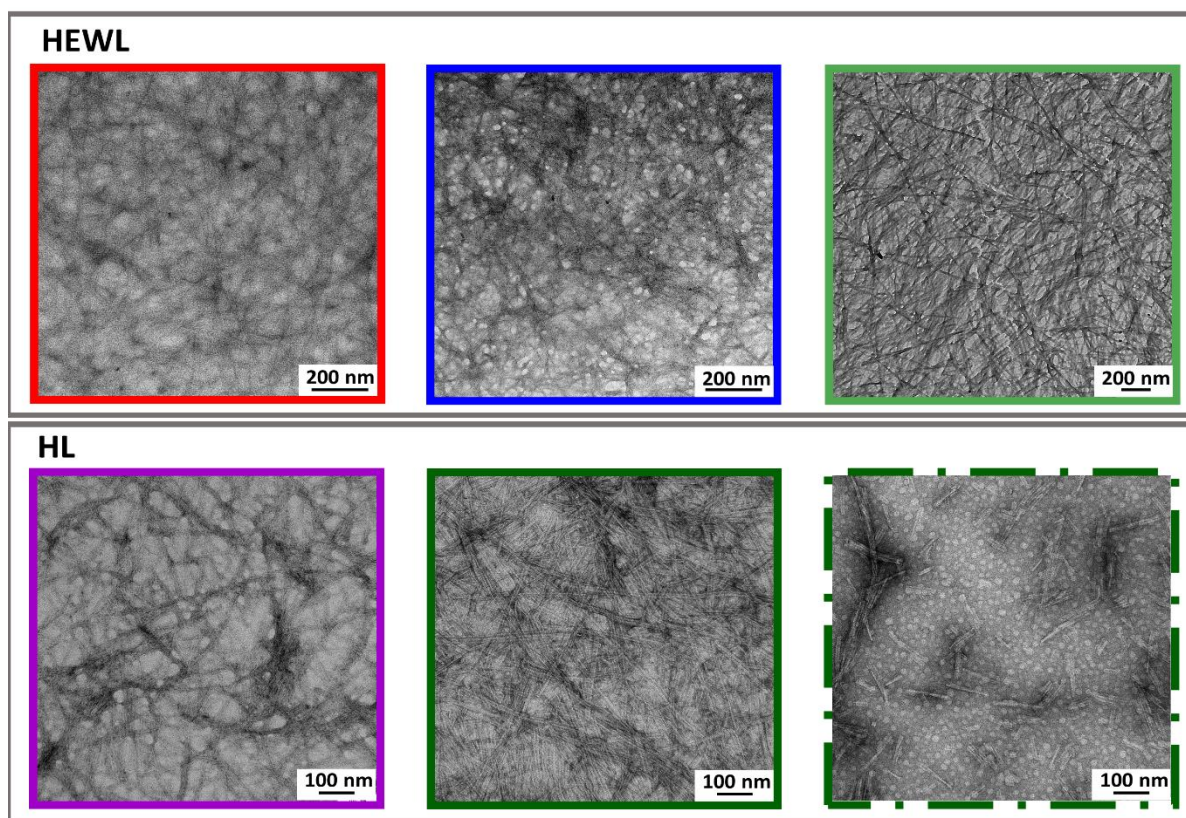


Fig. S2. TEM images of HEWL and HL prefibrillar states and fibrils. Protofibrils/fibrils were formed via incubation at 60°C of the aqueous HEWL solution of the initial concentration of 60 mg ml⁻¹ at pH 2.0 with agitation at 1400 rpm. HEWL: fibrils were captured due to recording spectra/images at different incubation times (3 (—), 5 (—) and 11 (—) hours, respectively). HL: fibrils were captured due to recording spectra/images at different incubation times (4 (—), 6 (—) and 8 (---) hours, respectively).

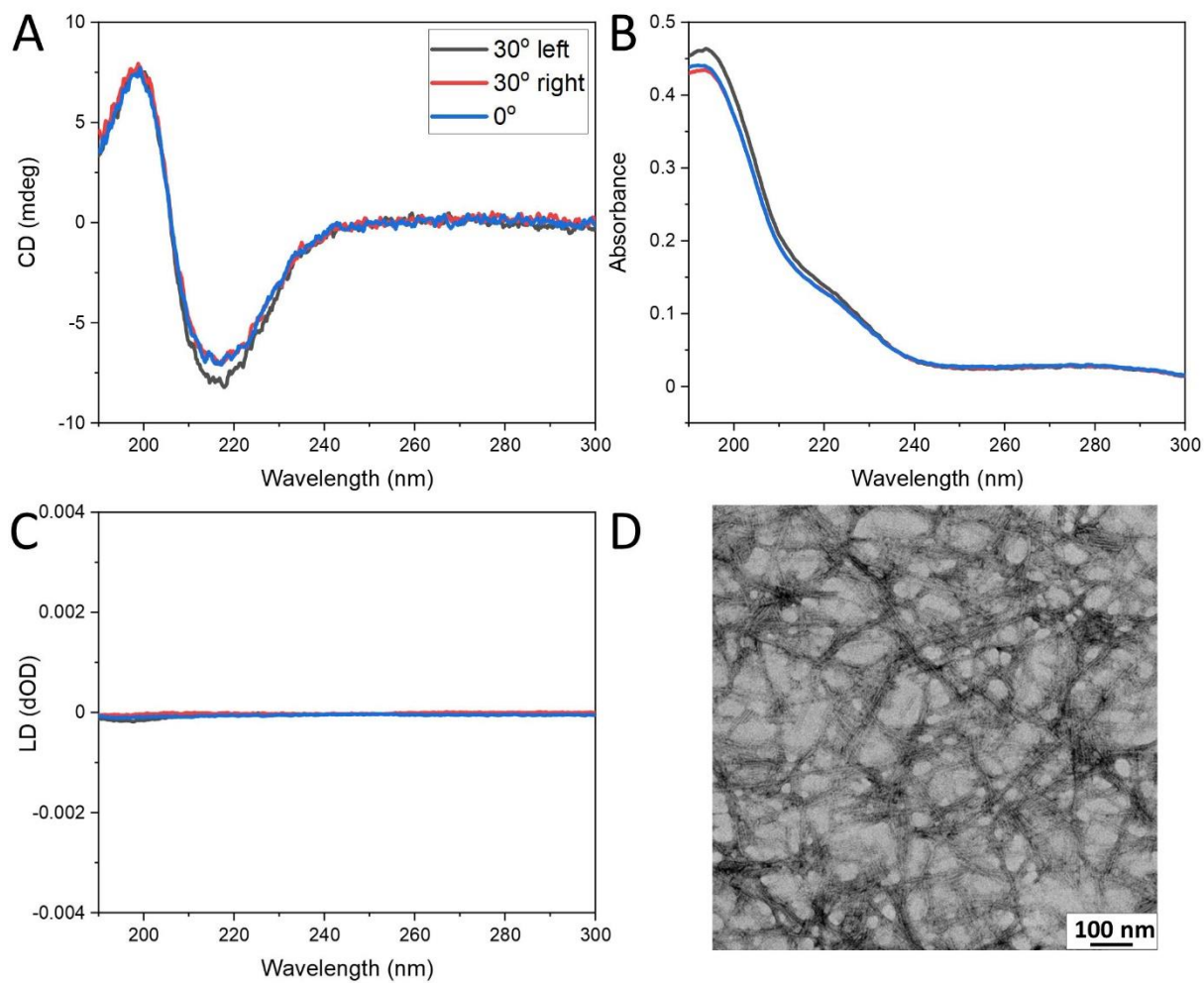


Fig. S3. Evaluation of anisotropy in fibril samples. The experiment was repeated for various incubation times and both for HEWL and HL fibrils. Here, a representative image of ECD (A) and electronic absorption (B) spectra obtained in various cuvette positions (the cuvette rotated perpendicularly to the light beam) and LD spectra (C) for mature HEWL fibrils are shown along with the TEM image (D). Fibrils obtained due to 8 h incubation.

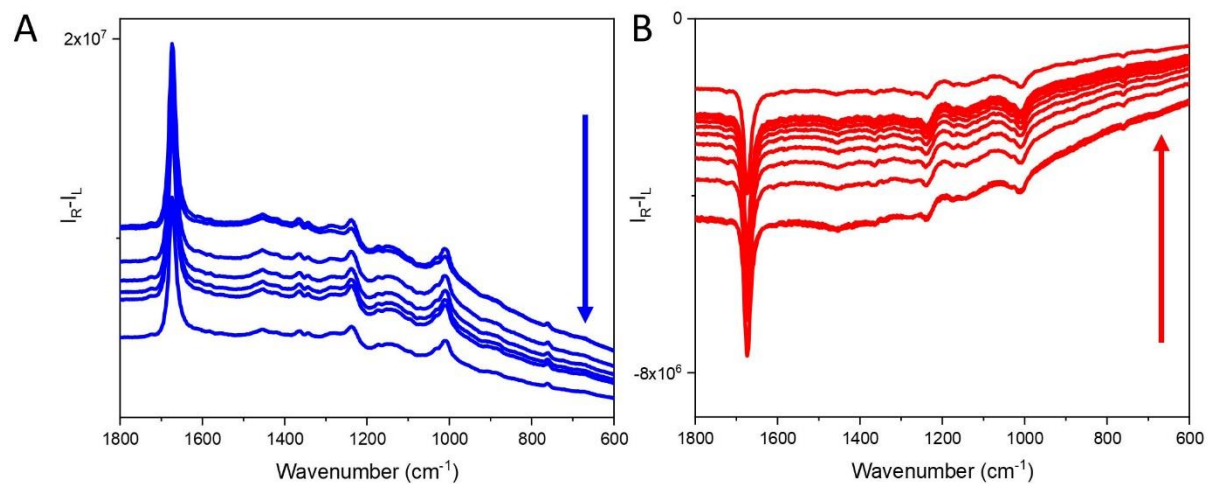


Fig. S4. Separate Raman and ROA spectral blocks for HEWL *early-stage* and *mature* fibrils: *early-stage* HEWL fibrils (5 h of incubation, **A**) and *mature* HEWL fibrils (11 h of incubation, **B**). The arrows show the decrease of the background with the time progress.

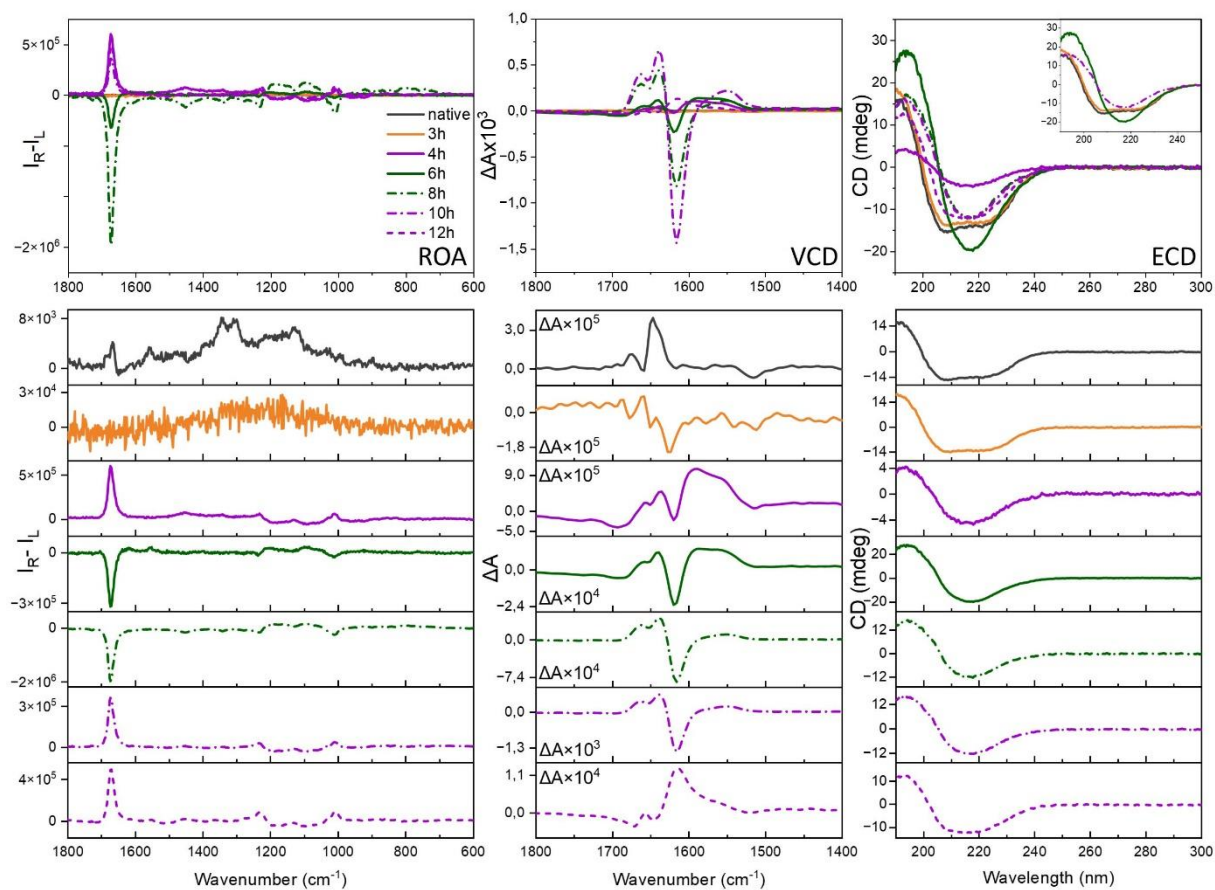


Fig. S5. Evolution of the ROA, VCD and ECD signals during formation of HL fibrils. For clarity, the selected ECD spectra are shown in the insert. Respective Raman, IR and electronic absorption spectra provided in Fig. S5.

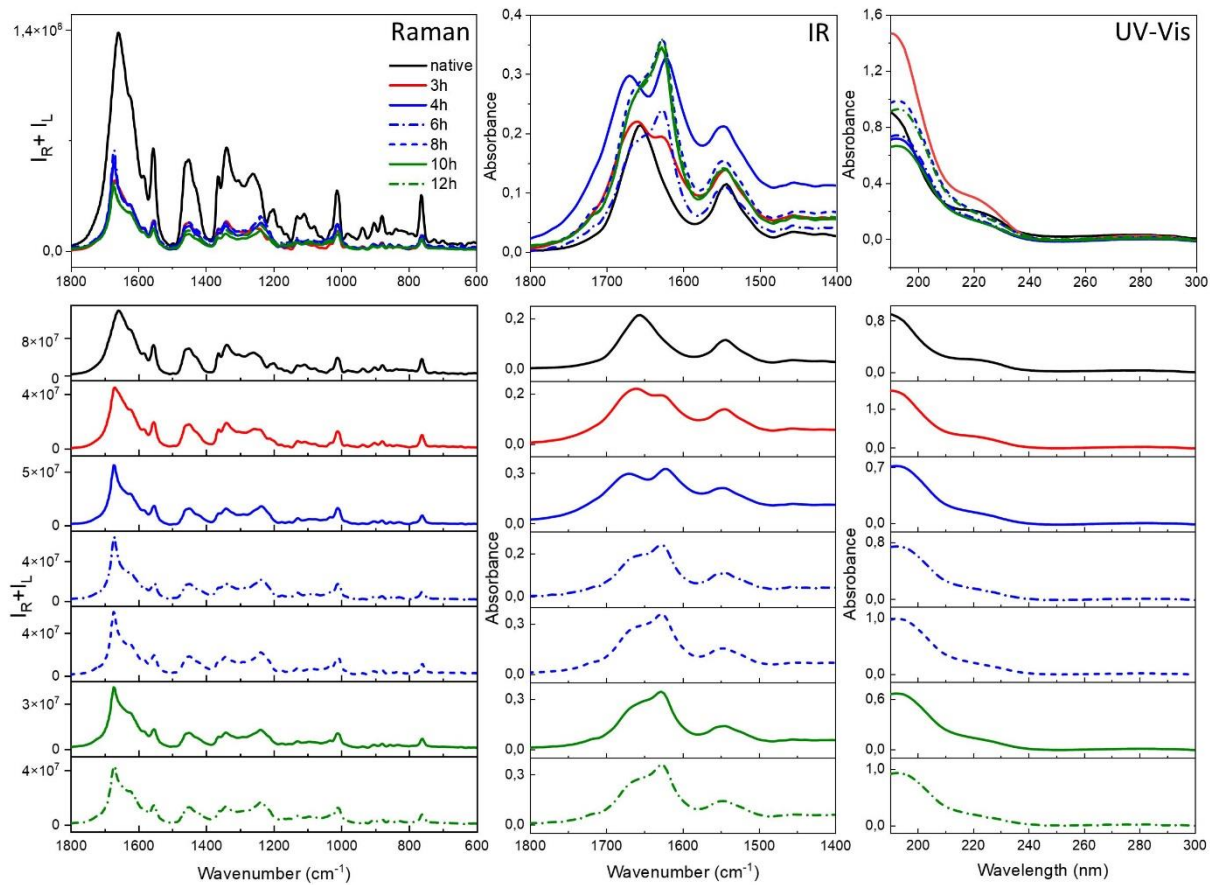


Fig. S6. Evolution of the Raman, IR and electronic absorption (UV-vis) spectra during HEWL formation.

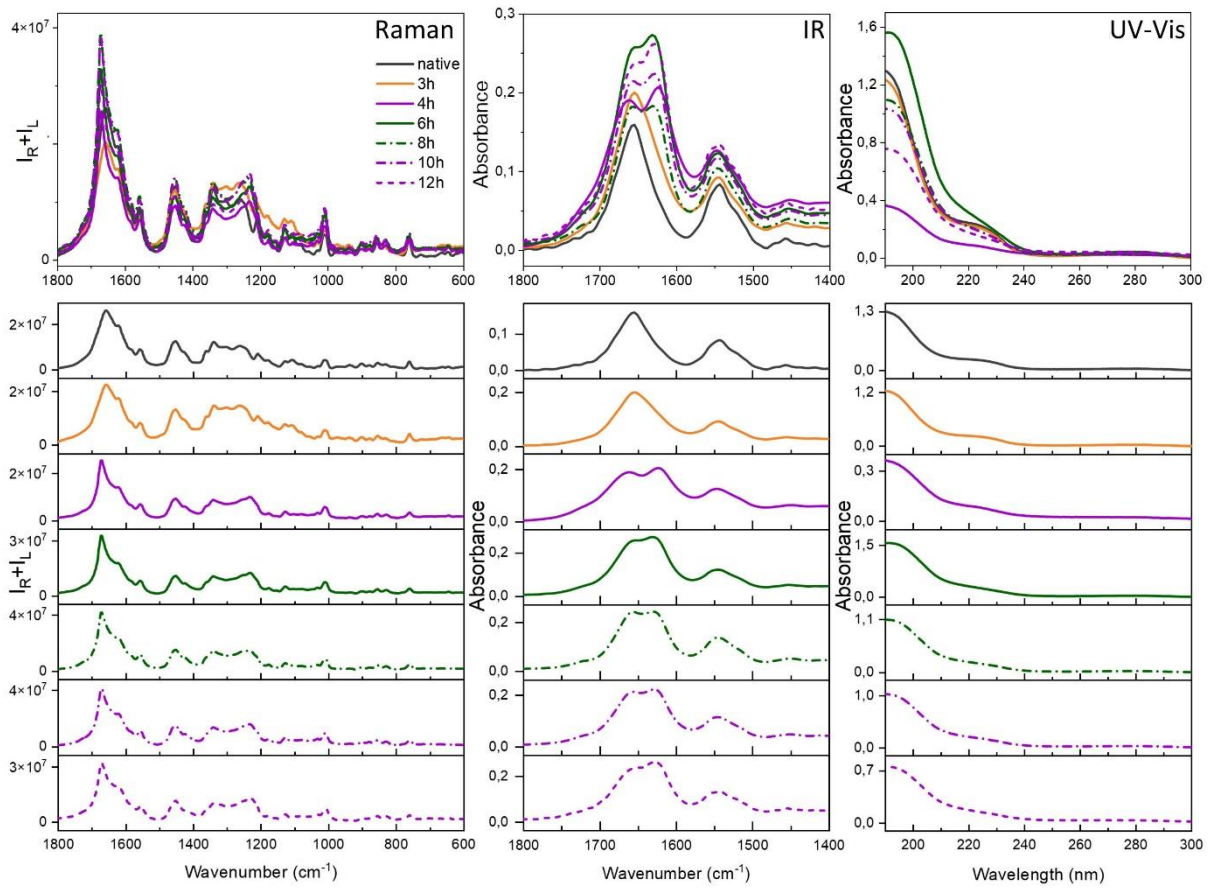


Fig. S7. Evolution of the Raman, IR and electronic absorption (UV-vis) spectra during HL formation.

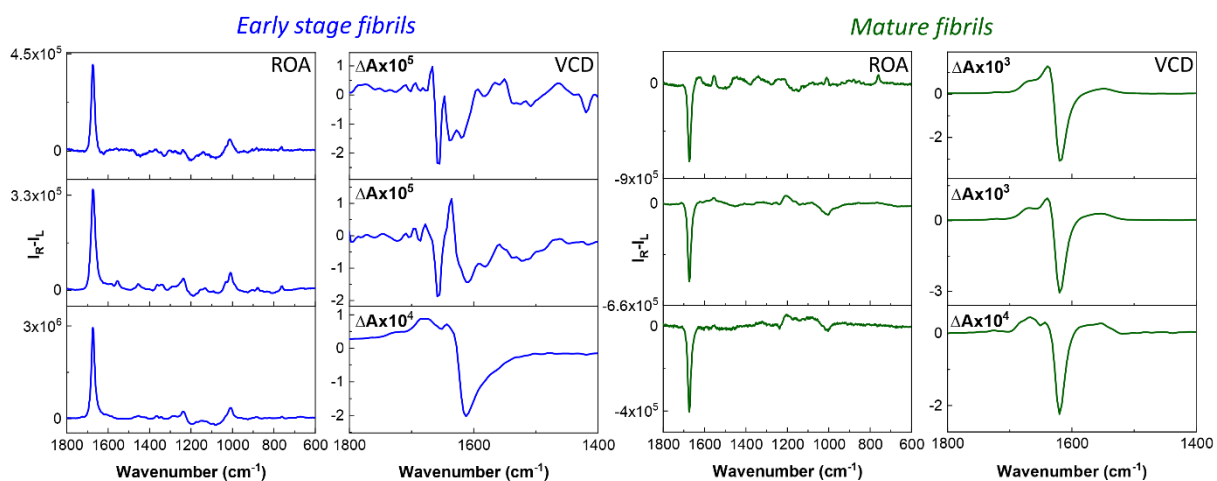


Fig. S8. Repetition of the time evolution experiment for HEWL. Early-stage and late-stage mature fibrils were formed via incubation at 60°C of the aqueous HEWL solution of the initial concentration of 60 mg ml⁻¹ at pH 2.0 with agitation at 1400 rpm.

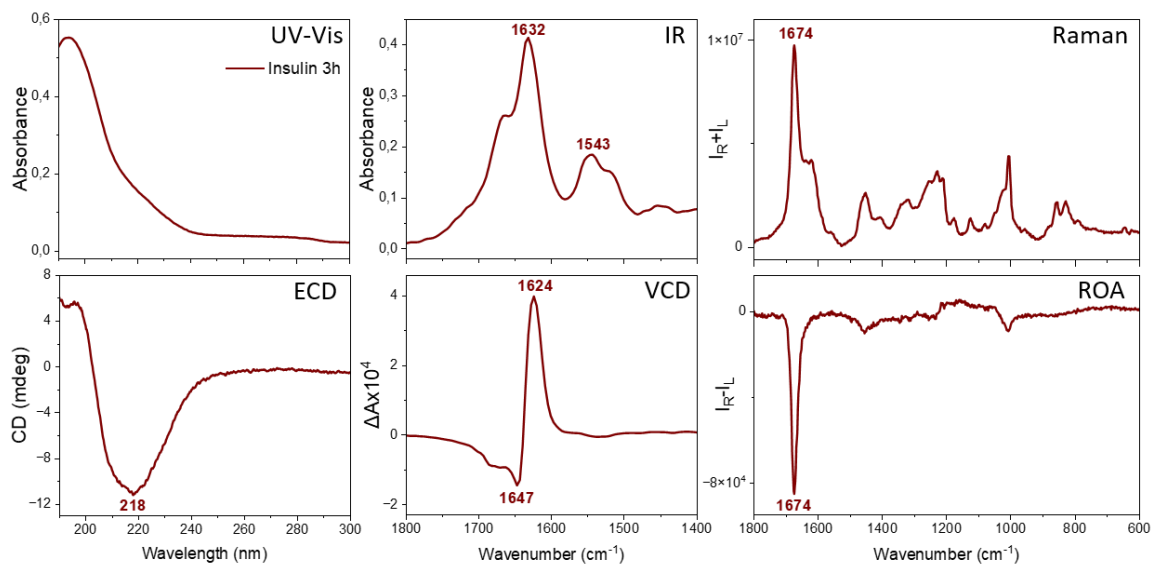


Fig. S9. Electronic absorption, IR, Raman, ECD, VCD and ROA spectra of mature insulin fibrils.

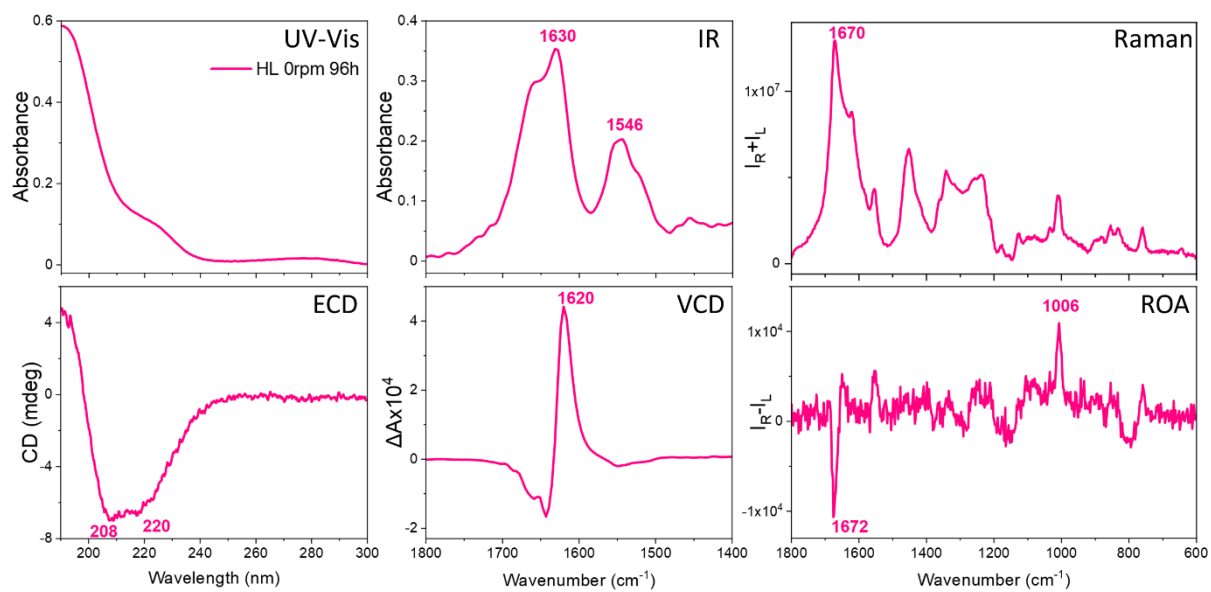


Fig. S10. Electronic absorption, IR, Raman, ECD, VCD and ROA spectra of HL fibrils obtained at the quiescent conditions.

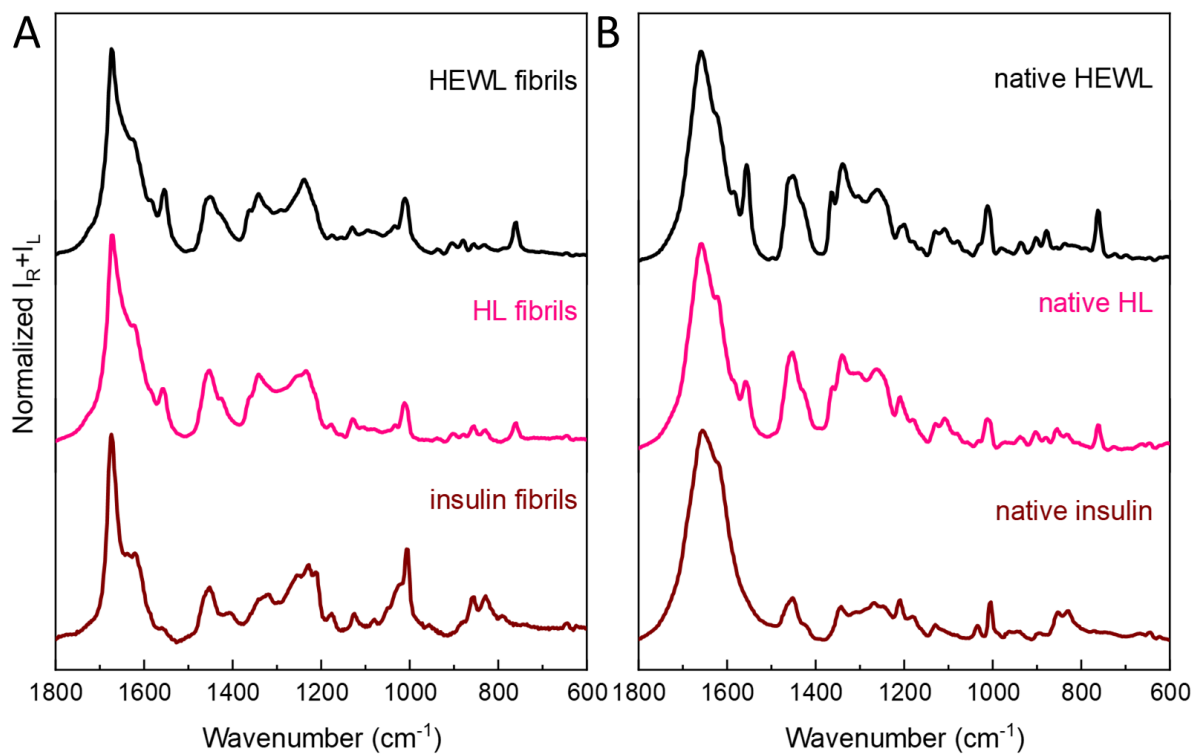


Fig. S11. Comparison of amyloid fibril Raman spectra (A): insulin (0 rpm), HEWL (1400 rpm) and HL (1400 rpm). Respective ROA spectra of native proteins are given for reference (B).

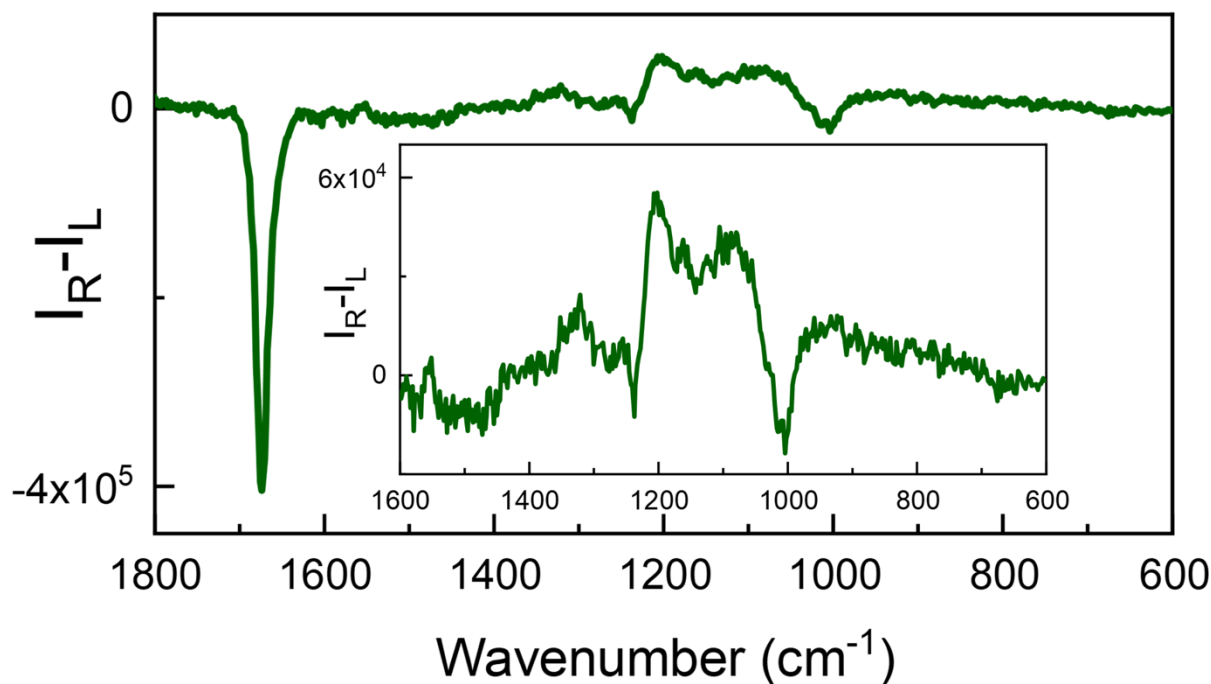


Figure S12. ROA of HEWL fibrils (10 h of incubation) with the inset showing more clearly the enhancement in the lower frequency range.

References

1. E. W. Blanch, L. A. Morozova-Roche, D. A. E. Cochran, A. J. Doig, L. Hecht and L. D. Barron, *J. Mol. Biol.*, 2000, 301, 553-563.
2. L. A. Morozova-Roche, J. Zurdo, A. Spencer, W. Noppe, V. Receveur, D. B. Archer, M. Joniau and C. M. Dobson, *J. Struct. Biol.*, 2000, 130, 339-351.
3. S. L. Ma, X. L. Cao, M. Mak, A. Sadik, C. Walkner, T. B. Freedman, I. K. Lednev, R. K. Dukor and L. A. Nafie, *J. Am. Chem. Soc.*, 2007, 129, 12364-12365.
4. N. Hachlica, M. Rawski, M. Górecki, A. Wajda, A. Kaczor, *Chem. Eur. J.*, 2023, 29, e202203827.
5. A. Micsonai, F. Wien, É. Bulyáki, J. Kun, É. Moussong, Y. H. Lee, Y. Goto, M. Réfrégiers and J. Kardos, *Nucleic Acids Res.*, 2018, 46, W315-W322.
6. A. Micsonai, F. Wien, L. Kernya, Y. H. Lee, Y. Goto, M. Réfrégiers and J. Kardos, *Proc. Natl. Acad. Sci. U.S.A.*, 2015, 112, E3095-E3103.
7. S. Yamamoto and H. Watarai, *Chirality*, 2012, 24, 97-103.
8. Polinski, L. A. Volpicelli-Daley, C. E. Sortwell, K. C. Luk, N. Cremades, L. M. Gottler, J. Froula, M. F. Duffy, V. M. Y. Lee, T. N. Martinez, K. D. Dave, *J. Parkinsons Dis.*, 2018, 8, 303.
9. F. Langer, Y. S. Eisele, S. K. Fritschi, M. Staufienbiel, L. C. Walker LC, M. Jucker, *J. Neurosci.*, 2011, 31, 14488-14495.
10. J. R. Silveira, G. J. Raymond, A. G. Hughson, R. E. Race, V. L. Sim, S. F. Hayes, B. Caughey, *Nature*, 2005, 437, 257-261.
11. G. Ghag, N. Bhatt, D. V. Cantu, M. J. Guerrero-Munoz, A. Ellsworth, U. Sengupta, R. Kaye, *Protein Sci.*, 2018, 27, 1901-1909.